First-principles thermodynamic theory of Seebeck coefficients

Yi Wang,[*] Yong-Jie Hu, Brandon Bocklund, Shun-Li Shang, Bi-Cheng Zhou, Zi-Kui Liu, and Long-Qing Chen[†]

Department of Materials Science and Engineering, The Pennsylvania State University, University Park, Pennsylvania 16802, USA

Thermoelectric effects, measured by the Seebeck coefficients, refer to the phenomena in which a temperature difference or gradient imposed across a thermoelectric material induces an electrical potential difference or gradient, and vice versa, enabling the direct conversion of thermal and electric energies. All existing first-principles calculations of Seebeck coefficients have been based on the Boltzmann kinetic transport theory. In this work, we present a fundamentally different method for the first-principles calculations of Seebeck coefficients without using any assumptions of the electron-scattering mechanism, being in contrast to the traditional theory by Cutler and Mott that shows the dependence of the Seebeck coefficient on the scattering mechanisms. It is shown that the Seebeck coefficient is a well-defined thermodynamic quantity that can be determined from the change in the chemical potential of electrons induced by the temperature change and thus can be computed solely based on the electronic density of states through first-principles calculations at different temperatures. The proposed approach is demonstrated using the prototype PbTe and SnSe thermoelectric materials.

I. INTRODUCTION

Thermoelectric effects refer to the phenomenon that a temperature gradient induces an electromotive force across a thermoelectric material and vice versa, enabling the direct conversion of thermal and electric energies. It has drawn unprecedented interests in the field of clean-energy technologies [1–4]. There have been extensive efforts in the search for thermoelectric materials with the best performances quantified by the figures of merit [5,6]

$$ZT = \frac{\sigma \alpha^2}{\kappa} T, \tag{1}$$

where σ is the electric conductivity, κ is the thermal conductivity, α is the Seebeck coefficient, and T is temperature.

Among the three physical quantities σ, κ, and α in Eq. (1), σ and κ are kinetic coefficients. It is more a challenge for the accurate calculations of the electronic conductivity and lattice thermal conductivity since the calculation of a kinetic quantity requires further knowledge of the scattering mechanism, which then depends on the knowledge of relaxation time and electron group velocity [7,8]. In the existing literature, the kinetic Boltzmann transport theory [7,9,10] is typically employed for determining the thermoelectric effects from first-principles calculations, relying on a further assumption of the mechanism of electron scattering, e.g., the constant relaxation time approximation.

Meanwhile, it has not been always clear whether the Seebeck coefficient can be defined purely from thermodynamics [11]. The main focus of this work is on the understanding and calculation of the Seebeck coefficient. We present a purely thermodynamic approach to computing the Seebeck

coefficient which is independent of scattering mechanisms, being different from the traditional method by Cutler and Mott [9] that shows the dependence of the Seebeck coefficient on the scattering mechanisms.

The Seebeck coefficient α in Eq. (1) measures the magnitude of the thermoelectric effect and is given by the ratio of the induced electric potential difference ($\Delta\phi$) to the imposed temperature difference (ΔT) across a thermoelectric material [12], i.e.,

$$\alpha = -\left(\frac{\Delta\phi}{\Delta T}\right)_p, \tag{2}$$

where the subscript p represents the pressure at which the thermoelectric coefficient is measured at zero current density, i.e., when the material is at thermodynamic equilibrium at constant pressure and an imposed temperature difference. When the temperature difference becomes infinitesimally small, the Seebeck coefficient becomes

$$\alpha = -\left(\frac{\partial\phi}{\partial T}\right)_P. \tag{3}$$

As a result, the Seebeck coefficient is a thermodynamic property represented by the derivative of electric potential (ϕ) with respect to the thermal potential (T).

II. THERMODYNAMIC THEORY OF THE SEEBECK COEFFICIENT

There are a number of existing attempts to define the Seebeck coefficient based on thermodynamics, and the earliest dates back to the work by Callen in 1948 [12]. For example, Wood [13] defined the Seebeck coefficient as the total derivative of the electrochemical potential of electrons with respect to temperature, which was later called the Kelvin formula by Peterson and Shastry [14], while changing the

---

*yuw3@psu.edu
†lqc3@psu.edu

total derivative into a partial derivative at constant volume. However, as pointed out by Apertet *et al.* [11], it is not clear whether the potential gradient in the Kelvin formula is the chemical potential or the electrochemical potential gradient. Furthermore, to our knowledge, all existing applications based on the Kelvin formula have been limited to model systems [11,14,15].

To understand the thermodynamic nature of the Seebeck coefficient, we can start by considering the charge carriers within a thermoelectric material as a thermodynamic system. The variation of the Gibbs free energy of the system with temperature and amount of charge carriers at constant pressure is given by

$$dG = -SdT + \mu dN, \quad (4)$$

where G is the Gibbs free energy of the charge-carrier system, S is entropy, μ is chemical potential, and N is the total number of charge carriers. The variation of the chemical potential with respect to temperature is simply related to the entropy per charge carrier, i.e.,

$$\partial \mu / \partial T = -\partial S / \partial N = -\theta. \quad (5)$$

Now we imagine that there are two pieces of the same thermoelectric solid but one at temperature T_1 and the other at temperature T_2, or there are two locations within the same thermoelectric solid with one location at temperature T_1 and the other at temperature T_2. There must be a difference in the chemical potentials of the charge carriers between these two pieces of solid or the two locations due to the temperature difference. This chemical potential difference can be converted to voltage difference just like in electrochemistry, i.e.,

$$\Delta \phi = \Delta \mu / q \quad \text{or} \quad d\phi = d\mu / q, \quad (6)$$

where q is the amount of charge per charge carrier with $-e$ (e is the amount of charge for one electron) for electrons and e for electron holes. As a result, the thermoelectric effect can be written as entropy per unit charge, i.e.,

$$\alpha = -\partial \phi / \partial T = -1/q \ \partial \mu / \partial T = \theta / q. \quad (7)$$

Therefore, the Seebeck coefficient α is purely a thermodynamic quantity defined in terms of two potentials, the electric potential ϕ and the thermal potential T or in terms of entropy per particle of charge carrier. It is easy to see that if the charge carriers are electrons, the Seebeck coefficient is negative, and if the charge carriers are electron holes, the Seebeck coefficient is positive since the entropy per charge carrier is always positive.

We can then formulate a relation between the electric potential ϕ in Eq. (3) and the chemical potential of electrons calculated using Mermin's finite-temperature extension of density-functional theory (DFT) [16,17] under the framework of the modern first-principles approach [18–23]. According to Ziman [24], the *absolute thermal electric force*, Θ, can be defined as

$$\Theta(T) = \int_0^T \alpha dt. \quad (8)$$

Since there are no other mobile charged species in the system except the electronic charge carriers, the difference in chemical potential of electrons due to the temperature difference must be the only thermodynamic source responsible for the electric potential difference. For a uniform material with uniform temperature, a temperature change results in the change in the chemical potential of thermal electrons, i.e., the temperature-dependent portion of the free-energy gain per electron. For a nonuniform system, each point in space can be considered as a thermodynamic system, and thus a system with a nonuniform temperature distribution has a nonuniform distribution of chemical potentials of electrons. The gradient in chemical potential of electrons is the thermodynamic driving force for electron transport.

By relating the Ziman equation [Eq. (8)] to the chemical potential of electrons, we propose to relate the absolute thermal electric force to the chemical potential of electrons,

$$\phi(T) = \frac{1}{q} \int_0^T \frac{\partial \mu(t)}{\partial t} dt = \frac{1}{q} [\mu(T) - \varepsilon_F] = \frac{1}{q} \zeta(T), \quad (9)$$

where $\mu(T)$ is the chemical potential of electrons (or Fermi level) by Mermin's theory [16,17] and ε_F is the Fermi energy. The notation of $\zeta = \mu - \varepsilon_F$ is reminiscent of that given by Sommerfeld [25], so that Eq. (9) sets $\phi = 0$ at 0 K. Following the previous calculations of the thermal electronic contribution to thermodynamic properties at finite temperatures [26,27] based on Mermin's theory [16,17], we can obtain the temperature dependence of chemical potential of electrons based on the electron density of states.

Considering the fact that the electrons are explicitly treated in the current implementation [21,22] of DFT, hereafter in all the formulations we will use $q = -e$. To obtain the Seebeck coefficient under Mermin's theory, we can start from the conservation equation

$$\int n(\varepsilon, V) f d\varepsilon = N, \quad (10)$$

where $n(\varepsilon, V)$ is the electronic density of states (e-DOS), N is the total number of electrons in the considered system, and f is the Fermi-Dirac distribution:

$$f = \frac{1}{\exp\left[\frac{\varepsilon + e\phi}{k_B T}\right] + 1}. \quad (11)$$

Here we note that in Eqs. (10) and (11), the Fermi energy ε_F has been taken as the reference for the band energy ε.

Finding the full derivative of Eq. (10) under the isobaric condition and noting that N is a constant and V is temperature dependent, we have

$$\left(\frac{\partial V}{\partial T}\right)_p \int \frac{\partial n(\varepsilon, V)}{\partial V} f d\varepsilon + \int n(\varepsilon, V) \frac{\partial f}{\partial T} d\varepsilon = 0, \quad (12)$$

with

$$\frac{\partial f}{\partial T} = \frac{1}{k_B} f(1 - f) \left[\frac{-e}{T}\left(\frac{\partial \phi}{\partial T}\right)_p + \frac{\varepsilon - \zeta}{T^2}\right]. \quad (13)$$

After a few rearrangements, we obtain the formulation to calculate the Seebeck coefficient under the isobaric

condition, α_P:

$$\alpha_P = -\left(\frac{\partial \phi}{\partial T}\right)_P = -\frac{k_B T \beta}{e\eta} \int \frac{\partial n(\varepsilon, V)}{\partial V} f\, d\varepsilon$$

$$- \frac{1}{eT\eta V} \int n(\varepsilon, V) f(1-f)(\varepsilon - \zeta)\, d\varepsilon, \quad (14)$$

where β is the volume thermal expansion coefficient and

$$\eta = \frac{1}{V} \int n(\varepsilon, V) f(1-f)\, d\varepsilon. \quad (15)$$

Equation (14) demonstrates that the Seebeck coefficient can be computed from the e-DOS instead of the electric conductivity used in the Boltzmann transport theory [9,28]. While e-DOS, $n(\varepsilon, V)$, is readily accessible from first-principles calculations [29–31], σ in Eq. (1) is a much more challenging quantity to compute, which requires the calculation of electron group velocity and the assumption of a constant relaxation time [32]. Therefore, the present formulation of Eq. (14) provides a straightforward computational method to calculate the Seebeck coefficient for thermoelectric materials employing first-principles calculations. The efficiency of the proposed approach in comparison with the kinetic Boltzmann transport theory (using the BOLTZTRAP package [10]) is given in the Appendix, Table I.

From Eq. (14), it is seen that the constant-pressure Seebeck coefficient contains two terms: one accounts for the thermal expansion contribution—-the first term on the right-hand side of Eq. (14), and the other accounts for the constant volume contribution—-the second term on the right-hand side of Eq. (14). Therefore, the effects of thermal expansion on the Seebeck coefficient are very similar to the classical case of constant-pressure heat capacity vs the constant-volume heat capacity. In the case of the Seebeck coefficient, the effects of thermal expansions can be described as the coupled effects of the volume dependence of the electronic density of states, together with temperature and volume expansion coefficients.

From the present approach, we can obtain the finite-temperature mobile charge-carrier concentration η in Eq. (15). The integral $\int n(\varepsilon, V) f(1-f)\, d\varepsilon$ can be considered as the total number of mobile carriers in a thermoelectric solid—-the number of electrons participating in the conduction process at finite temperature. This can be understood in the sense that the pair product of $f(1-f)$ represents the possibility that the electrons occupied "f number" of electronic states with energy ε, transmitted to (or vice versa), the "$1-f$ number" of unoccupied electronic states with energy ε at finite temperature. Accordingly, $n(\varepsilon, V)f(1-f)$ represents the density of states of charge carriers at finite temperature.

III. COMPARISON WITH THE BOLTZMANN TRANSPORT THEORY

A. Low-temperature limit

First, we can compare the present formulation with that derived from the kinetic Boltzmann transport theory [7,9,10] at the limit of $T \to 0$. Using Sommerfeld's low-temperature

expansion [25,33], we get

$$\phi = -\frac{\pi^2}{6e}(k_B T)^2 \left.\frac{\partial \ln n(\varepsilon, V)}{\partial \varepsilon}\right|_{\varepsilon=0}. \quad (16)$$

Therefore at $T \to 0$, we have

$$\alpha_V = -\frac{\pi^2 k_B^2 T}{3e} \left.\frac{\partial \ln n(\varepsilon, V)}{\partial \varepsilon}\right|_{\varepsilon=0}. \quad (17)$$

This relation tells that at the limit of $T \to 0$, a thermoelectric material is p type if its e-DOS has a negative slope at the Fermi energy with increasing band energy whereas it is n type if its e-DOS has a positive slope at the Fermi energy with increasing band energy. This is the situation for most insulators around the top of the valence band and the bottom of the conduction band.

On the other hand, for the Boltzmann transport theory [7,9,10] at the limit of $T \to 0$ [34]

$$\alpha_V = -\frac{\pi^2 k_B^2 T}{3e}\left[\left.\frac{\partial \ln \bar{n}(\varepsilon, V)}{\partial \varepsilon}\right|_{\varepsilon=\varepsilon_F}\right.$$
$$\left.+ \left.\frac{\partial \ln v^2(\varepsilon)}{\partial \varepsilon}\right|_{\varepsilon=\varepsilon_F} + \left.\frac{\partial \ln \tau(\varepsilon)}{\partial \varepsilon}\right|_{\varepsilon=\varepsilon_F}\right], \quad (18)$$

where $\bar{n}(\varepsilon, V) = n(\varepsilon - \varepsilon_F, V)$, v is an average electron velocity, and τ is the so-called relaxation time. In recent first-principles calculations [10,28,35–39], τ is mostly assumed to be constant. As pointed out by MacDonald [34], the constant τ approximation is just one of the choices at $T \to 0$. As a matter of fact, after using a correction for the free electrons with "screening" charge together with a constant mean-free path, instead of constant relaxation time, Wilson (see the book by MacDonald [34]) found that at $T \to 0$

$$\alpha_V = -\frac{\pi^2 k_B^2 T}{3e}\frac{1}{\varepsilon_F}, \quad (19)$$

with the parabolic band approximation [36] that $\bar{n}(\varepsilon) \propto \varepsilon^{1/2}$ and $v^2(\varepsilon) \propto \varepsilon$. Note that the evaluation of $\bar{n}(\varepsilon, V)$ in Eqs. (18) and (19) at $\varepsilon = \varepsilon_F$ is equivalent to evaluating $n(\varepsilon, V)$ in Eq. (17) at $\varepsilon = 0$.

B. Relation between the present formulation and the Boltzmann transport theory

By the Cutler-Mott theory [9], the Seebeck coefficient was formulated as

$$\alpha = \frac{1}{qT}\frac{\int [\varepsilon - \mu]\sigma(\varepsilon)\, d\varepsilon}{\int \sigma(\varepsilon)\, d\varepsilon}, \quad (20)$$

where $q = \pm e$ with the "−" sign for electrons as charge carriers and the "+" sign for holes, ε represents the electronic band energy, μ is the Fermi level, and $\sigma(\varepsilon)$ is a kinetic coefficient called the energy-dependent differential electrical conductivity.

By the Boltzmann transport theory [7], $\sigma(\varepsilon)$ in Eq. (20) can be calculated by

$$\sigma(\varepsilon) = e^2 f(1-f)\sum_{\mathbf{k}} \mathbf{v_k v_k}\tau_{\mathbf{k}}, \quad (21)$$

where $\mathbf{v_k}$ is the group velocity of the charge carriers with the crystal momentum $\mathbf{k}$. To relate the result from Eq. (20) using the Boltzmann transport theory to that from Eq. (14) (neglecting the effect of thermal expansion) using the present formulation, we can introduce an approximation by the Heisenberg uncertainty principle, such that $\mathbf{v_k}$ and τ in Eq. (18) approximately satisfy

$$\mathbf{v_k v_k}\tau = \frac{m_e \mathbf{v_k}}{m_e} \cdot \mathbf{v_k}\tau \propto \frac{\Delta \mathbf{p}\Delta \mathbf{l}}{m_e} \propto \frac{\hbar}{2m_e}\chi\left(\frac{T_0}{T}\right), \quad (22)$$

where m_e is the mass of electrons, $\hbar$ is the reduced Planck constant, and χ can be a function that only depends on temperature.

C. Incorporating the effect of thermal expansion to the Boltzmann transport theory

In case one insists on using the Boltzmann transport theory to calculate the Seebeck coefficient, the effect of thermal expansion can be included by

$$\alpha_p = -\frac{k_B T \beta}{e\eta} \int \frac{\partial n(\varepsilon, V)}{\partial V} f d\varepsilon$$
$$- \frac{1}{eT} \frac{\int [\varepsilon - \zeta] f(1-f) \sum_{\mathbf{k}} \mathbf{v_k v_k}\tau_{\mathbf{k}} d\varepsilon}{\int f(1-f) \sum_{\mathbf{k}} \mathbf{v_k v_k}\tau_{\mathbf{k}} d\varepsilon}. \quad (23)$$

Here, note that the reference point of the band energy ε has been shifted by treating the Fermi energy as the reference.

IV. COMPUTATIONAL DETAILS

The actual validation of the proposed formalism is carried out by performing first-principles calculations for the widely studied thermoelectric material PbTe [40,41] and the new thermoelectric material SnSe discovered by Zhao *et al.* [42–44]. For simplicity, we assume the rigid-band approximation [7], i.e., the band structure is assumed to remain unchanged from doping or from the thermal electronic excitation at finite temperatures. Therefore, a positive doping (*p* doping or hole doping) only shifts the Fermi energy toward a low energy, transforming the insulator into a *p*-type conductor even at 0 K. Similarly, a negative doping (*n* doping or electron doping) increases the Fermi energy above the (bottom) edge of the conduction band, transforming the insulator into an *n*-type conductor even at 0 K.

In the following we present the computational details for the first-principles calculations. One needs to first overcome several issues for the first-principles calculations. The major issue is concerned with the band gap, which is mostly underestimated by the commonly employed generalized gradient approximation [45] and local-density approximation [46]. Fortunately for PbTe, the pioneering calculations performed by Singh [47] showed that the Engel-Vosko generalized gradient approximation [48] plus spin-orbit coupling as implemented in WIEN2K package [23] gave an excellent band structure and reasonable band-gap values. Therefore, we followed Singh's work for the e-DOS calculation for both PbTe and SnSe. For the e-DOS calculation of PbTe using WIEN2K, we follow exactly the same settings by Singh, i.e., linearized augmented plane-wave sphere radii (R) of 2.9 bohr were used for both Pb and Te; $R \times k_{max} = 9.0$ where k_{max} is
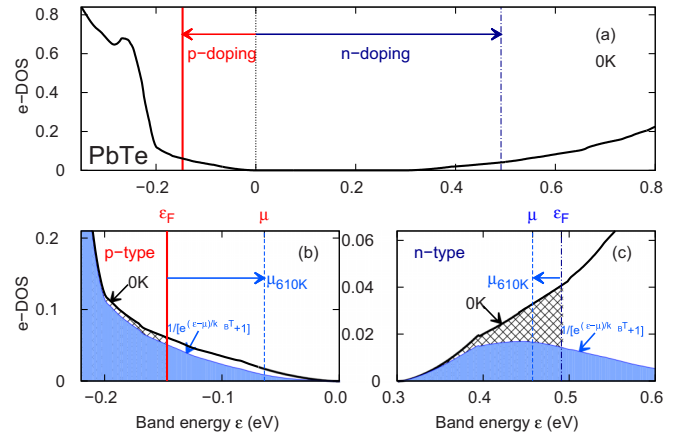

FIG. 1. Illustration of the Seebeck effect: (a) the calculated electronic density of states (black curve); the *p*-doping shifts the Fermi energy toward lower energy as indicated by the red arrow pointing to the left; the *n*-doping increases the Fermi energy as indicated by the blue arrow pointing to the right; (b) plot of electron density of states near the Fermi energy for *p* doping; (c) plot of electron density near the Fermi energy for *n* doping. (b), (c) The areas shaded by gray (partially overlapped by the blue shaded areas) represent the electron occupation at 0 K and the blue shaded areas indicate the electron occupation at a finite temperature of 610 K described by the Fermi distribution.

the interstitial plane-wave cutoff; and $48 \times 48 \times 48 \, k$ mesh. These settings, together with the Engel-Vosko generalized gradient approximation plus spin-orbit coupling, are the key to producing the band gap and e-DOS feature in the range $-0.35 \sim 0.0$ eV as shown in Fig. 1. For the e-DOS calculation of SnSe using WIEN2K, linearized augmented plane-wave sphere radii (R) of 2.5 bohr were used for both Sn and Se together with $R \times k_{max} = 7.0$ and $28 \times 26 \times 10 \, k$ mesh. The calculated band gap for SnSn is 0.61 eV, which is the same as that calculated by Zhao *et al.* [42]. In comparison, the reported experimental band gap for SnSe was 0.86 eV by Zhao *et al.* [42] while for $Ag_{0.01}Sn_{0.99}Se$ the band gap was experimentally estimated to be 0.5 eV by Chen *et al.* [49].

The second issue is concerned with the calculations of the lattice parameter as a function of temperature and the resulting thermal expansion. The good e-DOS from the Engel-Vosko generalized gradient approximation is at the cost of losing accuracy for the total energy. We overcame the problem by invoking the Perdew-Burke-Ernzerhof revised for solids (PBEsol) [50] exchange-correlational functional as implemented in the Vienna *Ab initio* Simulation Package (VASP, version 5.3) [21,22]. For PbTe, the Pb $5d^{10}6s^26p^2$ and Te $6s^26p^4$ electrons have been treated in the valence states; an energy cutoff of 336.7 eV and $20 \times 20 \times 20 \, k$ mesh was used for calculating the total energy. At room temperature, aided by the quasiharmonic phonon approximation, PBEsol provides a lattice parameter of 0.3242 nm which is within 0.3% of the experimental value of 0.3232 nm [11] for PbTe. For SnSe, the Sn $4d^{10}5s^25p^2$ and Se $5s^25p^4$ electrons were treated in the valence states; an energy cutoff of 336.7 eV and $18 \times 17 \times 7 \, k$ mesh was used for calculating the total energy. At room
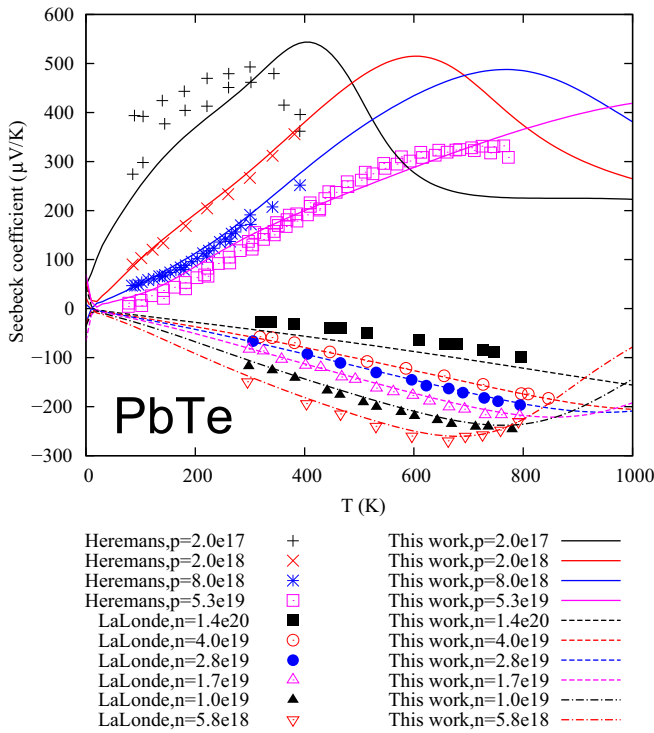
FIG. 2. The calculated Seebeck coefficients for PbTe for p-type doping levels of 2.0×10^{17}, 2.0×10^{18}, 8.0×10^{18}, and 5.3×10^{19} cm^{-3} and n-type doping levels of 1.4×10^{20}, 4.0×10^{19}, 2.8×10^{19}, 1.7×10^{19}, 1.0×10^{19}, and 5.8×10^{18} cm^{-3}. Corresponding to these number sequences, the lines represent the present calculations while the symbols (with same colors and sequences as the lines) represent the measured data for p-type PbTe by Heremans and coauthors [40,41] and n-type PbTe by LaLonde *et al.* [57].
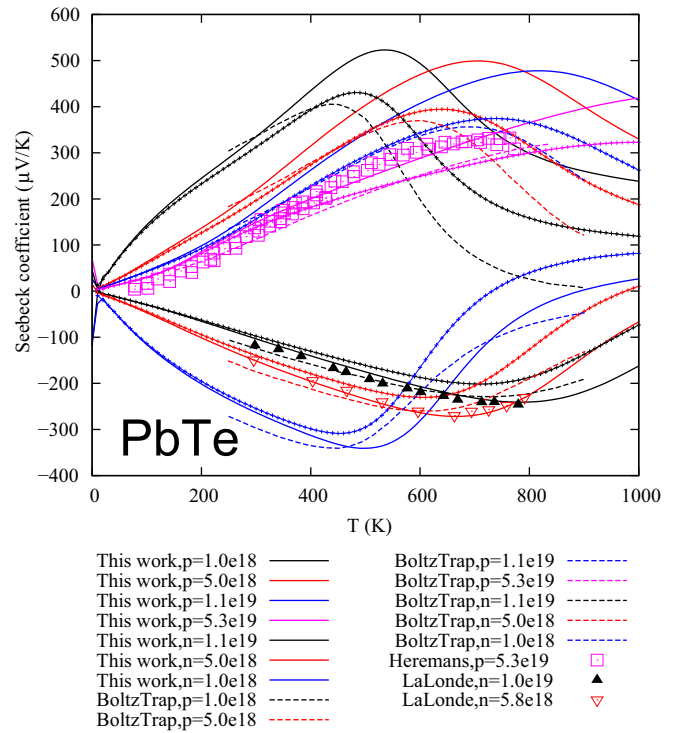
FIG. 3. Comparison among the present approach with considering the effects of thermal expansion (solid lines), the present approach without considering the effects of thermal expansion (solid lines marked by the cross signs), and Boltzmann transport theory (dashed lines). The dots represent the measured data at p-type doping levels of 5.3×10^{19} cm^{-3} by Heremans and coauthors [40,41] and n-type doping levels of 1.0×10^{19} and 5.8×10^{18} cm^{-3} by LaLonde *et al.* [57].

temperature, using the quasiharmonic phonon approximation, PBEsol results in lattice parameters of 0.4159, 0.4397, and 1.1469 nm, which are comparable to the experimental values of 0.4153, 0.4445, and 1.1501 nm [51] for SnSe.

The third issue is about the phonon calculation for polar insulators in order to obtain the finite-temperature thermodynamic properties. For this issue, the present authors have proposed a mixed-space approach [52–55] to account for the dipole-dipole interactions for a phonon calculation in the real space using the supercell method. The required inputs of Born effective charge and dielectric constant tensors to the mixed-space approach are calculated following the linear-response approach by Gajdoš *et al.* [56]. For PbTe, an energy cutoff of 237.8 eV and $3 \times 3 \times 3$ k mesh and a $4 \times 4 \times 4$ supercell containing 128 atoms were used for phonon calculation. For SnSe, an energy cutoff of 241.1 eV and $3 \times 3 \times 3$ k mesh and a $2 \times 2 \times 2$ supercell containing 54 atoms were used for phonon calculations.

V. NUMERICAL RESULTS AND DISCUSSION

Figure 1 illustrates the evolution of electron density of states and the corresponding chemical potential as a function of temperature in single-crystal PbTe. PbTe is an intrinsic semiconductor as indicated by its 0 K e-DOS shown in Fig. 1(a). Therefore, at 0 K, PbTe is an insulator since the

conduction band is unoccupied and separated by an energy gap from the completely filled valence band. As temperature increases, the electron occupation among electronic states changes. When the e-DOS curve has a negative slope at the 0 K Fermi energy with respect to the band energy as in the case of p-type PbTe shown in Fig. 1(a), i.e., there are fewer states for the electrons to occupy with increasing energy, the chemical potential of electrons will increase with increasing temperature as shown in Fig. 1(b). Similarly, when the e-DOS curve has a positive slope with increasing energy at the 0 K Fermi energy with respect to the band energy, i.e., there are more states for the electrons to occupy with increasing energy as in the case of n-type PbTe in Fig. 1(a), the chemical potential of electrons will decrease with increasing temperature as shown in Fig. 1(c).

Figure 2 compares the calculated Seebeck coefficients with measurements for PbTe at a variety of p- and n-doping levels. The minor difference between the calculated and measured data for the p-type doping levels of 2.0×10^{17} cm^{-3} could be due to the experimental uncertainty, while the slight difference between the calculated and measured data for the n-type doping levels of 1.4×10^{20} cm^{-3} could be due to the rigid-band approximation at high doping levels.

Figure 3, using PbTe as an example, shows the comparison among the present approach with considering the
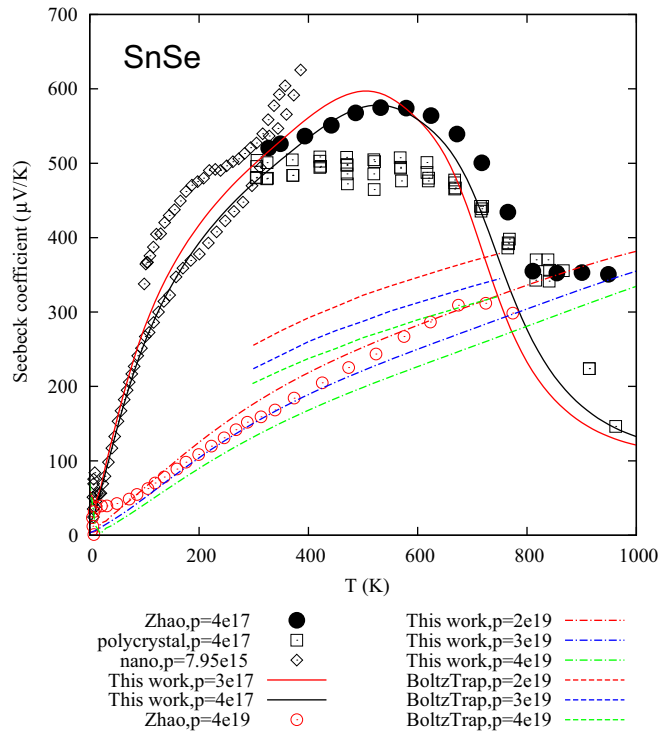
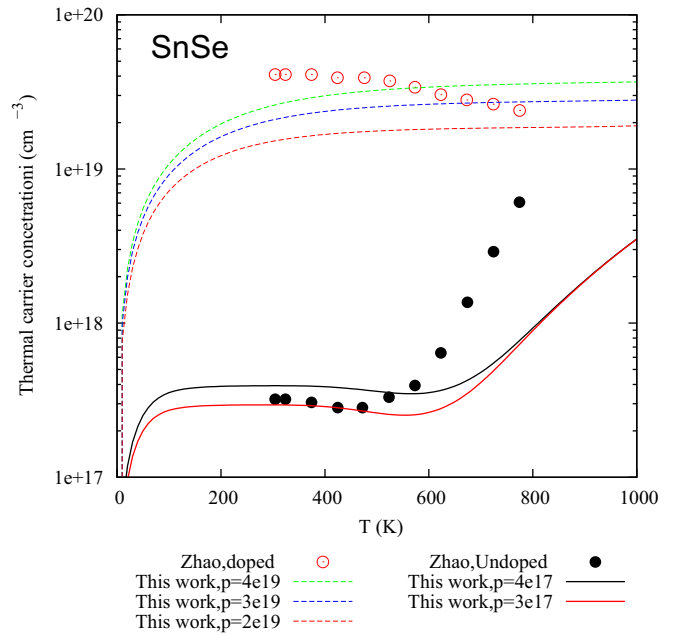FIG. 4. The calculated Seebeck coefficients for *p*-type SnSe compared with experiments [42,43,58,59].

FIG. 5. The mobile charge-carrier concentrations for *p*-type SnSe. The open and closed circles represent experimental data for *p*-type doping with nominated carrier concentrations, respectively, of $\sim 4 \times 10^{19}\,\mathrm{cm}^{-3}$ and $\sim 4 \times 10^{17}\,\mathrm{cm}^{-3}$, from Zhao *et al.* [42].

effects of thermal expansion (solid lines), without considering the effects of thermal expansion (solid lines marked by the cross signs), and Boltzmann transport theory (dashed lines, BOLTZTRAP [10] by Madsen and Singh), at the same *p*-type doping levels of 1.0×10^{18}, 5.0×10^{18}, and $1.1 \times 10^{19}\,\mathrm{cm}^{-3}$, and *n*-type doping levels of 1.1×10^{19}, 5.0×10^{18}, and $1.0 \times 10^{18}\,\mathrm{cm}^{-3}$. To support the comparison, also plotted in Fig. 3 are the available experimentally measured data with similar carrier concentrations at *p*-type doping levels of $5.3 \times 10^{19}\,\mathrm{cm}^{-3}$ by Heremans and coauthors [40,41] and *n*-type doping levels of 1.0×10^{19} and $5.8 \times 10^{18}\,\mathrm{cm}^{-3}$ by LaLonde *et al.* [57]. Without considering the effects of thermal expansion, it is indeed observed that the present approach produces very similar results with the kinetic approach by Singh [47]. With considering the effects of thermal expansion, the calculated Seebeck coefficient is increased by 10–20% at high temperature. In the moderate temperature range, the calculated Seebeck coefficients by the present approach have larger slopes than those calculated by Singh using BOLTZTRAP [10]. This is likely due to the fact that the thermal expansion effects were not accounted for in the BOLTZTRAP code. The same is observed for the calculated results for SnSe in Fig. 4.

Figure 4 illustrates the calculated Seebeck coefficients for *p*-type SnSe in comparison with the measured data for doped SnSe [42–44,58,59]. The calculations were performed at the *p*-type doping levels of 4×10^{19}, 3×10^{19}, and $2 \times 10^{19}\,\mathrm{cm}^{-3}$ to compare with Hall data of $4 \times 10^{19}\,\mathrm{cm}^{-3}$. The selection of these theoretical doping levels was based on the observations that for the nominated carrier concentration of

$4 \times 10^{19}\,\mathrm{cm}^{-3}$ by Zhao *et al.* [44], the measured carrier concentration has decreased from $\sim 4 \times 10^{19}$ to $\sim 2 \times 10^{19}\,\mathrm{cm}^{-3}$ at 800 K. Meanwhile, Zhao *et al.* [44] showed that for the measured Seebeck coefficients [42] with the nominated carrier concentration $\sim 4 \times 10^{17}\,\mathrm{cm}^{-3}$, the real carrier concentration is $\sim 3 \times 10^{17}\,\mathrm{cm}^{-3}$ at 300 K. To compare with the measured data for the undoped SnSe [42] with the nominated carrier concentration of $\sim 4 \times 10^{17}\,\mathrm{cm}^{-3}$, the calculations were performed at the *p*-type doping levels of 3×10^{17} and $4 \times 10^{17}\,\mathrm{cm}^{-3}$. The calculated mobile charge-carrier concentrations for *p*-type SnSe are illustrated in Fig. 5 and are in reasonable agreement with experimental data by Zhao *et al.* [42].

VI. CONCLUSION

In summary, this work provides an alternative theory to the traditional kinetic Boltzmann transport theory for the calculation of the Seebeck coefficient: (i) it demonstrates that the Seebeck coefficient is a well-defined thermodynamic quantity; (ii) the present work also provides a theoretical framework for taking into account the effects of thermal expansion on the Seebeck coefficient; and (iii) the present work provides a method for calculating the temperature-dependent carrier concentrations. Compared with the Boltzmann transport theory, the present framework does not require the parabolic-band approximation or the electron relaxation time. The formalism relies only on the e-DOS that is a routine output from most first-principles calculations in contrast to the commonly employed approach based on the

Boltzmann transport theory that requires the calculations of group velocity of electrons.

APPENDIX

TABLE I. The efficiency of the present approach in comparison with BOLTZTRAP (in seconds).[a]

Approach	PbTe[b]	SnSe[c]
This work	1.1	1.0
BOLTZTRAP	209.0	29.2

[a]For a fair comparison, the calculations were performed without considering the effects of thermal expansion, under the conditions of single fixed volume and p-type doping level of 1.0×10^{18} cm^{-3}, and in a temperature range of 0–1000 K with an increment of 10 K. For programming, the present approach is implemented using PYTHON 3.6 noting that BOLTZTRAP code was in FORTRAN90.

[b]For BOLTZTRAP, the calculation was performed using $48 \times 48 \times 48$ k mesh in the reciprocal space. For the present work, the calculations were performed based on the electronic density of states made of 34 463 energy points accounting for all valence electrons.

[c]For BOLTZTRAP, the calculation was performed using $28 \times 26 \times 10$ k mesh in the reciprocal space. For the present work, the calculations were performed based on the electronic density of states made of 20 001 energy points accounting for all valence electrons.

[1] I. Vaskivskyi, J. Gospodaric, S. Brazovskii, D. Svetin, P. Sutar, E. Goreshnik, I. A. Mihailovic, T. Mertelj, and D. Mihailovic, Sci. Adv. **1**, e1500168 (2015).

[2] W. G. Zeier, J. Schmitt, G. Hautier, U. Aydemir, Z. M. Gibbs, C. Felser, and G. J. Snyder, Nat. Rev. Mater. **1**, 16032 (2016).

[3] C. Goupil, W. Seifert, K. Zabrocki, E. Müller, and G. J. Snyder, Entropy **13**, 1481 (2011).

[4] G. J. Snyder and E. S. Toberer, Nat. Mater. **7**, 105 (2008).

[5] K. Biswas, J. He, I. D. Blum, C.-I. Wu, T. P. Hogan, D. N. Seidman, V. P. Dravid, and M. G. Kanatzidis, Nature (London) **489**, 414 (2012).

[6] Y. Pei, X. Shi, A. LaLonde, H. Wang, L. Chen, and G. J. Snyder, Nature (London) **473**, 66 (2011).

[7] T. J. Scheidemantel, C. Ambrosch-Draxl, T. Thonhauser, J. V Badding, and J. O. Sofo, Phys. Rev. B **68**, 125210 (2003).

[8] G. D. Mahan and J. O. Sofo, Proc. Natl. Acad. Sci. **93**, 7436 (1996).

[9] M. Cutler and N. F. Mott, Phys. Rev. **181**, 1336 (1969).

[10] G. K. H. Madsen and D. J. Singh, Comput. Phys. Commun. **175**, 67 (2006).

[11] Y. Apertet, H. Ouerdane, C. Goupil, and P. Lecoeur, Eur. Phys. J. Plus **131**, 1 (2016).

[12] H. B. Callen, Phys. Rev. **73**, 1349 (1948).

[13] C. Wood, Rep. Prog. Phys. **51**, 459 (1988).

[14] M. R. Peterson and B. S. Shastry, Phys. Rev. B **82**, 195105 (2010).

[15] J. Hejtmánek, Z. Jirák, and J. Šebek, Phys. Rev. B **92**, 125106 (2015).

[16] A. K. McMahan and M. Ross, Phys. Rev. B **15**, 718 (1977).

[17] N. D. Mermin, Phys. Rev. **137**, A1441 (1965).

[18] P. Giannozzi, S. Baroni, N. Bonini, M. Calandra, R. Car, C. Cavazzoni, D. Ceresoli, G. L. Chiarotti, M. Cococcioni, I. Dabo, A. Dal Corso, S. de Gironcoli, S. Fabris, G. Fratesi, R. Gebauer, U. Gerstmann, C. Gougoussis, A. Kokalj, M. Lazzeri, L. Martin-Samos, N. Marzari, F. Mauri, R. Mazzarello, S. Paolini, A. Pasquarello, L. Paulatto, C. Sbraccia, S. Scandolo, G. Sclauzero, A. P. Seitsonen, A. Smogunov, P. Umari, and R. M. Wentzcovitch, J. Phys.: Condens. Matter **21**, 395502 (2009).

[19] X. Gonze, B. Amadon, P.-M. Anglade, J.-M. Beuken, F. Bottin, P. Boulanger, F. Bruneval, D. Caliste, R. Caracas, M. Côté, T. Deutsch, L. Genovese, P. Ghosez, M. Giantomassi, S. Goedecker, D. R. Hamann, P. Hermet, F. Jollet, G. Jomard, S. Leroux, M. Mancini, S. Mazevet, M. J. T. Oliveira, G. Onida, Y. Pouillon, T. Rangel, G.-M. Rignanese, D. Sangalli, R. Shaltaf, M. Torrent, M. J. Verstraete, G. Zerah, and J. W. Zwanziger, Comput. Phys. Commun. **180**, 2582 (2009).

[20] S. J. Clark, M. D. Segall, C. J. Pickard, P. J. Hasnip, M. I. J. Probert, K. Refson, and M. C. Payne, Z. Kristallogr. - Cryst. Mater. **220**, 567 (2005).

[21] G. Kresse and J. Furthmüller, Comput. Mater. Sci. **6**, 15 (1996).

[22] G. Kresse and D. Joubert, Phys. Rev. B **59**, 1758 (1999).

[23] P. Blaha, K. Schwarz, G. Madsen, D. Kvasnicka, and J. Luitz, *WIEN2k, An Augmented Plane Wave Plus Local Orbitals Program for Calculating Crystal Properties*, 2nd ed. (Vienna University of Technology, Vienna, 2001).

[24] J. M. Ziman, *Electrons and Phonons: The Theory of Transport Phenomena in Solids* (Clarendon, Oxford, 1960).

[25] A. Sommerfeld, *Thermodynamics and Statistical Mechanics* (Academic, New York, 1964).

[26] Y. Wang, J. J. Wang, H. Zhang, V. R. Manga, S. L. Shang, L. Q. Chen, and Z. K. Liu, J. Phys.: Condens. Matter **22**, 225404 (2010).

[27] Y. Wang, D. Chen, and X. Zhang, Phys. Rev. Lett. **84**, 3220 (2000).

[28] P. Reddy, S.-Y. Jang, R. A. Segalman, and A. Majumdar, Science **315**, 1568 (2007).

[29] A. Jain, S. P. Ong, G. Hautier, W. Chen, W. D. Richards, S. Dacek, S. Cholia, D. Gunter, D. Skinner, G. Ceder, and K. A. Persson, APL Mater. **1**, 011002 (2013).

[30] S. P. Ong, W. D. Richards, A. Jain, G. Hautier, M. Kocher, S. Cholia, D. Gunter, V. L. Chevrier, K. A. Persson, and G. Ceder, Comput. Mater. Sci. **68**, 314 (2013).

[31] S. Bhattacharya and G. K. H. Madsen, Phys. Rev. B **92**, 085205 (2015).

[32] L. D. Hicks and M. S. Dresselhaus, Phys. Rev. B **47**, 12727 (1993).

[33] K. Behnia, *Fundamentals of Thermoelectricity* (Oxford University Press, United Kingdom, 2015).

[34] D. K. C. MacDonald, *Thermoelectricity: An Introduction to the Principles* (John Wiley & Sons, Inc., New York, 1962).

[35] J. E. Parrott, IEEE Trans. Electron Devices **43**, 809 (1996).

[36] U. Sivan and Y. Imry, Phys. Rev. B **33**, 551 (1986).

[37] L. Gravier, S. Serrano-Guisan, F. Reuse, and J.-P. Ansermet, Phys. Rev. B **73**, 024419 (2006).

[38] M. Jonson and G. D. Mahan, Phys. Rev. B **21**, 4223 (1980).

[39] M. Jonson and G. D. Mahan, Phys. Rev. B **42**, 9350 (1990).

[40] J. P. Heremans, V. Jovovic, E. S. Toberer, A. Saramat, K. Kurosaki, A. Charoenphakdee, S. Yamanaka, and G. J. Snyder, Science **321**, 554 (2008).

[41] J. P. Heremans, C. M. Thrush, and D. T. Morelli, Phys. Rev. B **70**, 115334 (2004).

[42] L.-D. Zhao, S.-H. Lo, Y. Zhang, H. Sun, G. Tan, C. Uher, C. Wolverton, V. P. Dravid, and M. G. Kanatzidis, Nature (London) **508**, 373 (2014).

[43] L.-D. Zhao, G. Tan, S. Hao, J. He, Y. Pei, H. Chi, H. Wang, S. Gong, H. Xu, V. P. Dravid, C. Uher, G. J. Snyder, C. Wolverton, and M. G. Kanatzidis, Science **351**, 141 (2016).

[44] L.-D. Zhao, C. Chang, G. Tan, and M. G. Kanatzidis, Energy Environ. Sci. **9**, 3044 (2016).

[45] J. P. Perdew, K. Burke, and M. Ernzerhof, Phys. Rev. Lett. **77**, 3865 (1996).

[46] J. P. Perdew and A. Zunger, Phys. Rev. B **23**, 5048 (1981).

[47] D. J. Singh, Phys. Rev. B **81**, 195217 (2010).

[48] E. Engel and S. H. Vosko, Phys. Rev. B **47**, 13164 (1993).

[49] C.-L. Chen, H. Wang, Y.-Y. Chen, T. Day, and G. J. Snyder, J. Mater. Chem. A **2**, 11171 (2014).

[50] J. P. Perdew, A. Ruzsinszky, G. I. Csonka, O. A. Vydrov, G. E. Scuseria, L. A. Constantin, X. Zhou, and K. Burke, Phys. Rev. Lett. **100**, 136406 (2008).

[51] K. Adouby, C. Pérez-Vicente, J. C. Jumas, R. Fourcade, and A. A. Touré, Z. Kristallogr. - Cryst. Mater. **213**, 343 (1998).

[52] Y. Wang, J. J. Wang, W. Y. Wang, Z. G. Mei, S. L. Shang, L. Q. Chen, and Z. K. Liu, J. Phys.: Condens. Matter **22**, 202201 (2010).

[53] Z. K. Liu and Y. Wang, *Computational Thermodynamics of Materials* (Cambridge University Press, Cambridge, UK, 2016).

[54] Y. Wang, S. L. Shang, Z. K. Liu, and L. Q. Chen, Phys. Rev. B **85**, 224303 (2012).

[55] Y. Wang, S.-L. Shang, H. Fang, Z.-K. Liu, and L.-Q. Chen, npj Comput. Mater. **2**, 16006 (2016).

[56] M. Gajdoš, K. Hummer, G. Kresse, J. Furthmüller, and F. Bechstedt, Phys. Rev. B **73**, 045112 (2006).

[57] A. D. LaLonde, Y. Pei, G. J. Snyder, J. Zhang, B. Ren, Z. Wang, M. G. Kanatzidis, M. G. Kanatzidis, K. M. Paraskevopoulos, and M. G. Kanatzidis, Energy Environ. Sci. **4**, 2090 (2011).

[58] S. Sassi, C. Candolfi, J.-B. Vaney, V. Ohorodniichuk, P. Masschelein, A. Dauscher, and B. Lenoir, Appl. Phys. Lett. **104**, 212105 (2014).

[59] F. Serrano-Sánchez, M. Gharsallah, N. M. Nemes, F. J. Mompean, J. L. Martínez, and J. A. Alonso, Appl. Phys. Lett. **106**, 083902 (2015).